

Feature-based Lateral Position Estimation of Surrounding Vehicles Using Stereo Vision

Elijah S. Lee and Dongsuk Kum, *Member, IEEE*

Abstract— Driver behavior Prediction has become an important topic in the recent development of Advanced Driver Assistance Systems (ADAS). To predict future behavior and potential risks associated with surrounding vehicles, their lateral position information is required. However, existing computer vision algorithms tend to either focus on longitudinal measurements or provide lateral position information with limited performance for limited scenes (i.e no viewpoint change and occlusion). In this paper, feature-based lateral position estimation algorithm is proposed using stereo vision and provides lateral position regardless of viewpoint change and occlusion by extracting a pixel-wise feature. In the preprocessing step, v-disparity from stereo depth map is calculated and used for ground detection. Then, vehicle candidates are created based on image thresholding and filtering, removing the ground portion from the camera image. These generated candidates are verified as vehicles by using deep convolutional neural network. In order to track and estimate the lateral position of the detected vehicles, speeded up robust feature (SURF) points are matched in consecutive image frames, and the feature point is projected onto the ground; defined as the grounded feature point. Finally, inverse perspective mapping (IPM) is applied on the original image to estimate the lateral position of the grounded feature point. The proposed algorithm successfully detects a feature point of neighboring vehicle and estimates its lateral position by tracking the grounded feature point. For testing the algorithm, the datasets in a highway and an urban setting are used and provide zero mean error and 0.25m standard deviation error in lateral position estimation.

I. INTRODUCTION

Each year more than one million people around the world die due to road accidents, and most fatal traffic accidents involve more than one vehicle. Many commercial products with collision avoidance systems have been developed, and these Advanced Driver Assistance Systems (ADAS) aid drivers for improved safety and convenience. One particular risky scenario of interest is lane-changing of vehicles. Acknowledging lane change of surrounding vehicles ahead of time reduces accident rates because drivers can react and reduce the speed of ego vehicle. According to an article, vehicle lateral velocity is the most discriminant feature for lane change recognition [1]. That is, accurately measuring lateral position of surrounding vehicles is required to predict lane changes and possibly other important driver intentions. In fact, recent research shows that vehicle lateral position history can predict its future lateral motion with high accuracy [2].

E. S. Lee is with the Mechanical Technology Research Center, KAIST, Daejeon 305-701, Republic of Korea (e-mail: elijah4rain@kaist.ac.kr).

D. Kum is with the Cho Chun Shik Graduate School for Green Transportation, KAIST, Daejeon 305-701, Republic of Korea (corresponding author, e-mail: dskum@kaist.ac.kr).

Automotive industry has developed various sensors capable of detecting surrounding vehicles and their dynamic states. However, in nature, radar suffers from low accuracy in measuring lateral position, and only camera and lidar can provide reliable lateral information [3], [4]. Among these two candidates, camera is often considered a practical solution owing to its affordable cost and easy accessibility. In fact, camera can be fused with radar to improve lateral resolution of radar in detecting vehicle's lateral position [3], [5], [6].

In large, there are two challenges in tracking lateral position of neighboring vehicles with vision-based system. First, it is challenging to decide which part of a vehicle the vision sensor should detect in keeping track of lateral positions. In general, once the target for vehicle detection is set, particular shape or edge is to be extracted on the image frame. For instance, if an algorithm aims to detect vehicle license plate, a rectangular box is detected to indicate the vehicle position. In the literature, vision sensor mostly detects vehicle rear by using a bounding box [6], [7], [8]. For instance, aspect ratio of 1.2 is used in [7] while another uses square or half square as a bounding box [8]. However, this method does not provide accurate lateral position because a bounding box is detected based on overall image feature inside the box so it cannot perceive subtle lateral movement in pixels. Another approach detects vehicle centerlines by finding symmetric axis [5], [9]. This method is found to be robust in finding lateral position, but symmetric axis may not be found all the time. Other works include vehicle boundary detection by contour [10] and vehicle body detection by cuboid [11], but these techniques are much affected by noise in computing lateral motion. Therefore, selecting robust detection platform is necessary for accurate lateral position estimation.

The second problem statement is that the proposed system must estimate the lateral position of nearby vehicles regardless of viewpoint change and occlusion. Once the vehicle part to be tracked is decided on the first statement, the natural following question would be if the selected part can always be detected. The aforementioned bounding box approach usually extracts vehicle feature from the full image of the rear, which makes it challenging to detect vehicles with only portion of the rear shown on the camera image. To overcome this problem, Garcia et al. used optical flow for overtaking vehicle detection [12]. Optical flow detects the apparent motion of objects even for occluded vehicle parts, but the detection is not valid for static objects and it is hard to estimate vehicle lateral motion. Strode et al. presented multi-part vehicle detection using active learning and symmetry [8]. The learning algorithm trains half and full view of the vehicle rear part so a vehicle can be found even when the portion of the rear is invisible. However, this system relies on the bounding box approach, which cannot provide accurate lateral motion information.

In this paper, a feature-based algorithm that estimates vehicle lateral position regardless of viewpoint change and occlusion is proposed. This work focuses on detecting distinctive feature point, which can be found on even partially occluded vehicles regardless of viewpoint. With a help of stereo vision, the selected feature point on the vehicle is projected onto the ground, which defines the grounded feature point. Measuring the lateral position of the grounded feature point enables the estimation of vehicle lateral position. To the best of authors' knowledge, this is the first vision-based approach on measuring lateral position of surrounding vehicle regardless of viewpoint and occlusion. Feature-based system benefits from tracking in pixels and thus becomes an effective tool in estimating lateral position with robustness to noise.

II. OVERVIEW OF THE PROPOSED ALGORITHM

As Fig. 1 illustrates, the framework of the proposed lateral position estimation algorithm consists of four parts. First, image preprocessing is performed on the image data from stereo rig to build v-disparity map [13] for ground detection. Then, vehicle hypothesis generation based on thresholding and clustering gives vehicle candidates. In hypothesis verification, the vehicle candidates are verified as possible vehicles by using deep convolutional neural network, and the output with high score on Support Vector Machine (SVM) is considered a vehicle. As the final step, speeded up robust feature (SURF) points are matched on the detected vehicle from consecutive frames, and the feature point is projected onto the ground plane with a help of stereo vision's disparity map. The pixel coordinate of the grounded feature point is transferred to the ground using the inverse perspective mapping (IPM) so that the lateral position is estimated on the ground coordinate. The remainder of this paper is structured as

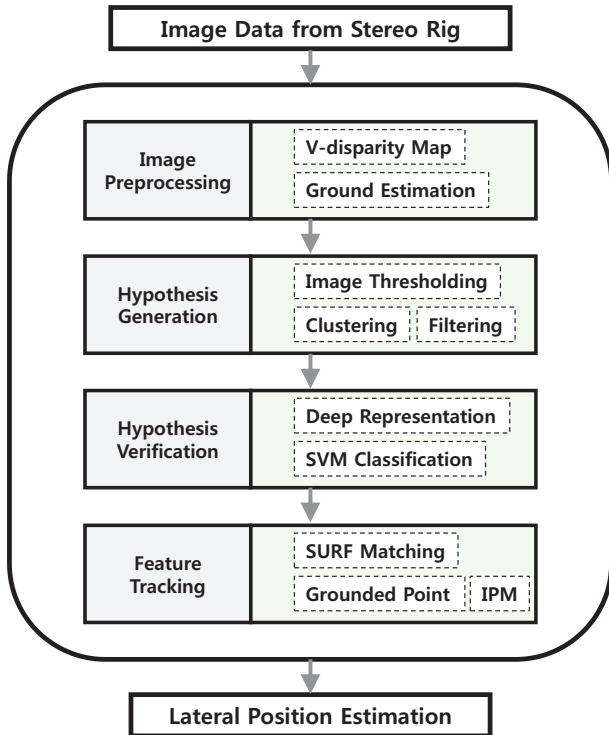


Figure 1. Framework of the proposed lateral position estimation algorithm given image data from stereo rig.

follows. Section III describes the main algorithm in vehicle detection and how the feature point tracking algorithm is formulated. Section IV presents experimental results of feature point detection and lateral position estimation. Concluding remarks are provided in Section V.

III. VEHICLE DETECTION AND FEATURE TRACKING

This section describes the overall vehicle detection scheme and newly introduces feature-based lateral position estimation method. As for the first part of the section, vision-based vehicle detection procedure is explained. Fig. 2 illustrates the overall vehicle detection process from the raw image data to the detected vehicles. The second part focuses on feature detection from the detected vehicles, and the grounded feature point is defined to estimate lateral position.

A. Vehicle Candidate Generation using V-disparity Map

Vehicle detection has been an interesting research topic and studied in many research community [3], [4], [14], [15]. In particular, stereo vision-assisted vehicle detection is known to be effective in depth estimation and also used for Advanced Driver Assistance System (ADAS) [16], [17]. As the first step of vehicle detection, the image data from stereo rig is used to create the depth map, as shown in Fig. 3. Each pixel of the depth map has disparity value, which is larger for closer distance. Accumulating the intensities over horizontal direction results in v-disparity map, and a hough line fit of the map can be obtained, as shown on the right side of Fig. 3. Then, the slope and y-intercept variation of the line fit over

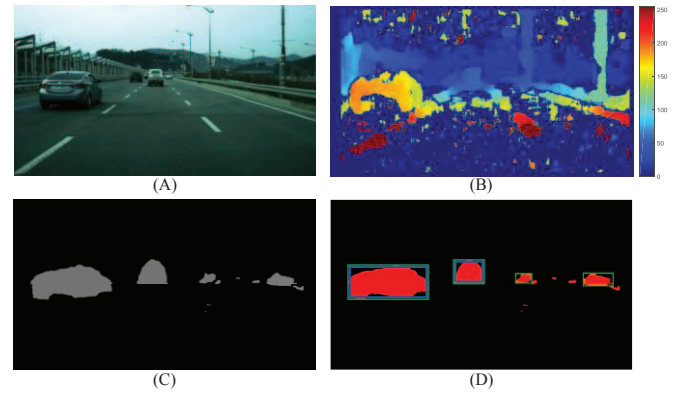


Figure 2. Overview of vehicle detection process. (A) Original image input. (B) Depth map with colorbar. (C) Object clustering from ground detection. (D) Vehicle candidates (green box) and verified vehicle (blue box).

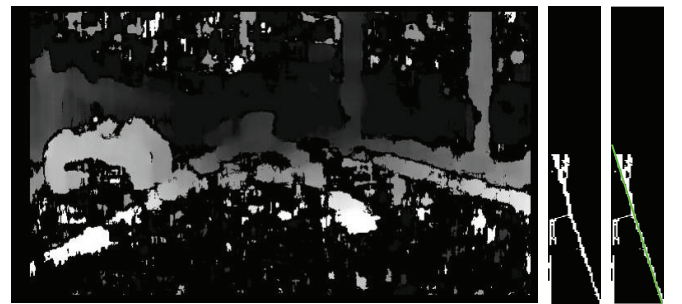


Figure 3. V-disparity map for ground detection. The depth image (left) is used to create v-disparity map (middle), and hough line fit (right) of the disparity map detects the ground (marked in green).

period of time are collected to provide the ground information, which is to be used in the later step of the proposed algorithm. Once ground is detected, obstacles can be extracted from the image by thresholding and filtering. These objects are then boxed in order to generate vehicle hypothesis candidates to be verified.

B. Vehicle Hypothesis Verification

Since the vehicle candidates collected from the previous step may include various viewpoints, conventional detection scheme such as bounding box approach would fail. In this work, deep learning-based verification method is proposed to solve this problem. In [18], authors use Deep Convolutional Neural Networks (DCNN) to generate vehicle candidates, which are then verified as vehicles by stereo vision. The DCNN shows high accuracy in detecting vehicles regardless of viewpoint and occlusion. Similarly, this work implements the DCNN but with SVM as the final classifier. Stereo vision is limited to tell if the detected object is guardrail or vehicle, and thus the proposed work confirms vehicle presence by selecting the output of high score from SVM classification. Moreover, the recent result shows that the higher layers of DCNN trained on a large dataset can be general enough for different dataset classification [19]. This technique transfers network parameters and presents high accuracy on classification task. As an example, vehicle classification using this transferable feature is performed and proven to outweigh the state of the art performance [20].

The vehicle candidate verification architecture is depicted in Fig. 4. VGG-M model [21] is employed for pre-trained CNN because VGG model demonstrates good performance on image classification with relatively fast speed. The input image first goes through five convolution (conv) layers, then enters two fully-connected (fc) layers, and proceeds to dimension reduction performed by Principal Component Analysis (PCA) to present the final SVM classification score. The labels on the convolution layers represent the number of convolution filters and their receptive field size, and the labels of fully-connected layers indicate their dimensionality. The transfer learning in this work trains over 7000 positive and negative images mainly from GTI dataset [22] for testing.

C. Feature Matching and Tracking

After the vehicle detection process, distinctive feature points from consecutive frames are matched and tracked for

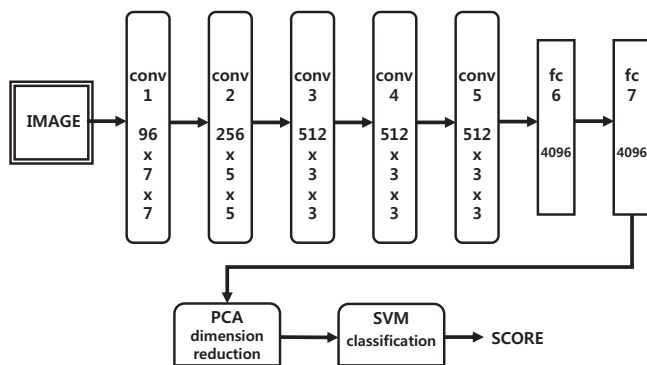


Figure 4. The structure of vehicle verification model. The input image enters deep convolutional networks, and SVM classification score is returned as an output after dimension reduction by PCA.

lateral position estimation. Fig. 5 illustrates sample images of the overall scheme for this stage. It is important to note that two cases are considered for feature matching. The first case is when the matched feature lies on the side part of vehicle, and the other is when the feature matching is done on the rear. This division helps the system detect the features in various viewpoints and also work for partially occluded vehicles.

To robustly detect a feature point, selecting distinctive feature is necessary. One widely used feature extraction method is Scale Invariant Feature Transform (SIFT), which is a distinctive invariant features that can perform reliable matching between different views of an object [23]. SIFT matching, however, requires a high computational cost, and thus a feature matching method with relatively lower computational cost, namely Speeded-Up Robust Features (SURF) [24], is used in this study. SURF is speeded-up version of SIFT and previously used for vehicle rear light status recognition [9]. SURF is only initially used to detect a salient feature, and the found feature is then tracked by the Kanade-Lucas-Tomasi (KLT) algorithm [25]. The KLT is a good pixelwise tracker, and Luvizon et al. uses the KLT algorithm to track feature points on vehicle license plate [26]. Let I_t and I_{t+1} be the consecutive image frames. According to the KLT algorithm, for given x as the feature point, the corresponding window ω is found by minimizing the error

$$E = \sum_{\omega} [I_t(x) - I_{t+1}(x + \vec{d})]^2 \quad (1)$$

where \vec{d} informs the feature motion between the two frames.

D. Grounded Feature Point Formation

After establishing the framework for feature tracking, there still must be an algorithm that correlates feature point motion with vehicle lateral motion. Since the lateral motion is easily observable from top view, the original camera image (Fig. 5(A)) is converted into a top view image (Fig. 5(D))

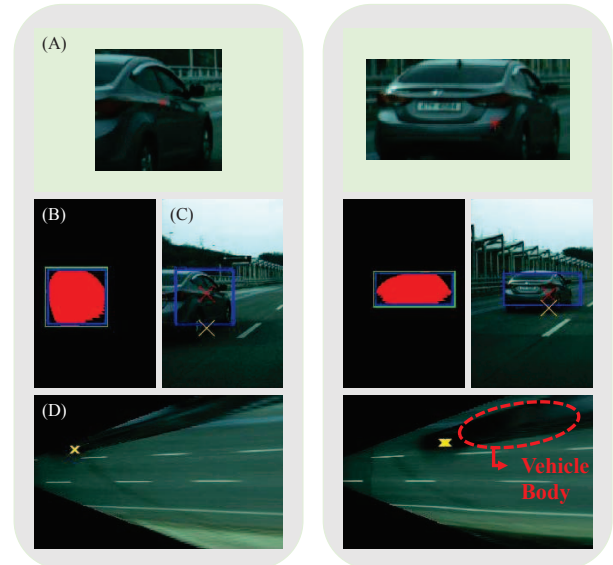


Figure 5. Overview of feature matching and tracking process. Two cases are shown: when the feature points are matched on the side part of vehicle (left) and when the feature points are matched on the rear (right). (A) SURF matching on the vehicle. (B) detected vehicle cluster from the previous step. (C) The matched feature point (red x) projection onto the ground (yellow x). (D) Grounded feature point transformation via Inverse Perspective Mapping.

using inverse perspective mapping (IPM) [27]. However, the SURF matched point is located somewhere on the vehicle body of the original image, which is above the ground, so the feature point would be transferred to some point of the top view image inside the region representing the vehicle body, as can be seen in Fig. 5. Any transferred point by this procedure would not provide the real vehicle lateral position, so the proposed work first projects the feature point onto the ground, defined as grounded feature point (yellow x in Fig. 5(C)), and then applies inverse perspective mapping to transfer the grounded feature point onto the top view image (yellow x in Fig. 5(D)). Tracking lateral position of this point will provide vehicle lateral position.

In order to account for the feature point projection onto the ground, schematic and pseudocode are provided in Fig. 6 and Fig. 7 for grounded feature point formation algorithm. The goal of the algorithm is to project a feature point $P_{feature}$ onto the ground, defined as grounded feature point P_{ground} . Fig. 6(A) shows that there are two possible cases where $P_{feature}$ is placed on the camera image (Fig. 6(B)). If $P_{feature}$ is placed on the vehicle side, P_{ground} will be on the solid green line in Fig. 6(A), and if $P_{feature}$ is on the rear, P_{ground} will be on the dotted blue line in Fig. 6(A)). Thus, the performance of algorithm relies on accurate approximation of these lines, denoted $line\ l$. The basic idea is to use y-intercept and slope information of ground estimation and find a collection of points near ground to find $line\ l$ as the line fit of those points. First, step 1 to 13 of algorithm 1 select two collection of points inside N_{down} by N rectangle that are above the ground, denoted as P_{left} and P_{right} (Fig. 6(C)). Then, step 14 to 20 select the lowest α number of points (cyan points in Fig. 6(D)) from P_{left} and P_{right} , and find $line\ l$ by line fitting of the α points that are closer. Step 16 compares the summation of Y values of the two α points groups, and the lower points on the image (P_{right} in Fig. 6(D))

Algorithm 1. Grounded Feature Point Formation

Input: Depth Map(D), Feature Point($P_{feature}$), Y-intercept(Y_{int}) and Slope(M) of ground line fit in V disparity map

```

1:  $P_{left} \leftarrow \{\}, P_{right} \leftarrow \{\}$ 
2: for  $i \leftarrow 1$  to  $N$ 
3:    $P \leftarrow i$  th left point of  $P_{feature}$ 
4:   for  $j \leftarrow 1$  to  $N_{down}$ 
5:      $P_{down} \leftarrow j$  th lower point of  $P$ 
6:      $D_{ground} \leftarrow \frac{P_{down}[2] - Y_{int}}{M}$ 
7:      $D_{map} \leftarrow$  disparity value of  $D$  at  $P_{down}$ 
8:     if  $D_{ground} < D_{map}$ 
9:        $P_{left} \leftarrow P_{left} \cup P_{down}$ 
10:    end if
11:  end for
12: end for
13: repeat step 2 to 12 for right side to obtain  $P_{right}$ 
14:  $S_{left} \leftarrow \sum(Y \text{ values of the lowest } \alpha \text{ points from } P_{left})$ 
15:  $S_{right} \leftarrow \sum(Y \text{ values of the lowest } \alpha \text{ points from } P_{right})$ 
16: if  $S_{left} < S_{right}$ 
17:    $l \leftarrow$  line fit of the lowest  $\alpha$  points from  $P_{right}$ 
18: else
19:    $l \leftarrow$  line fit of the lowest  $\alpha$  points from  $P_{left}$ 
20: end if
21:  $l' \leftarrow$  vertical line passing through  $P_{feature}$ 
22: return  $l \cap l'$ 

```

Output: Grounded Feature Point(P_{ground})

Figure 7. Grounded feature point formation algorithm.

are used for the line fit since they correspond to vehicle part closer to the camera, which provide more accurate estimation for depth map. Finally, step 21 to 22 return P_{ground} by finding the intersection point of $line\ l$ and vertical line through $P_{feature}$.

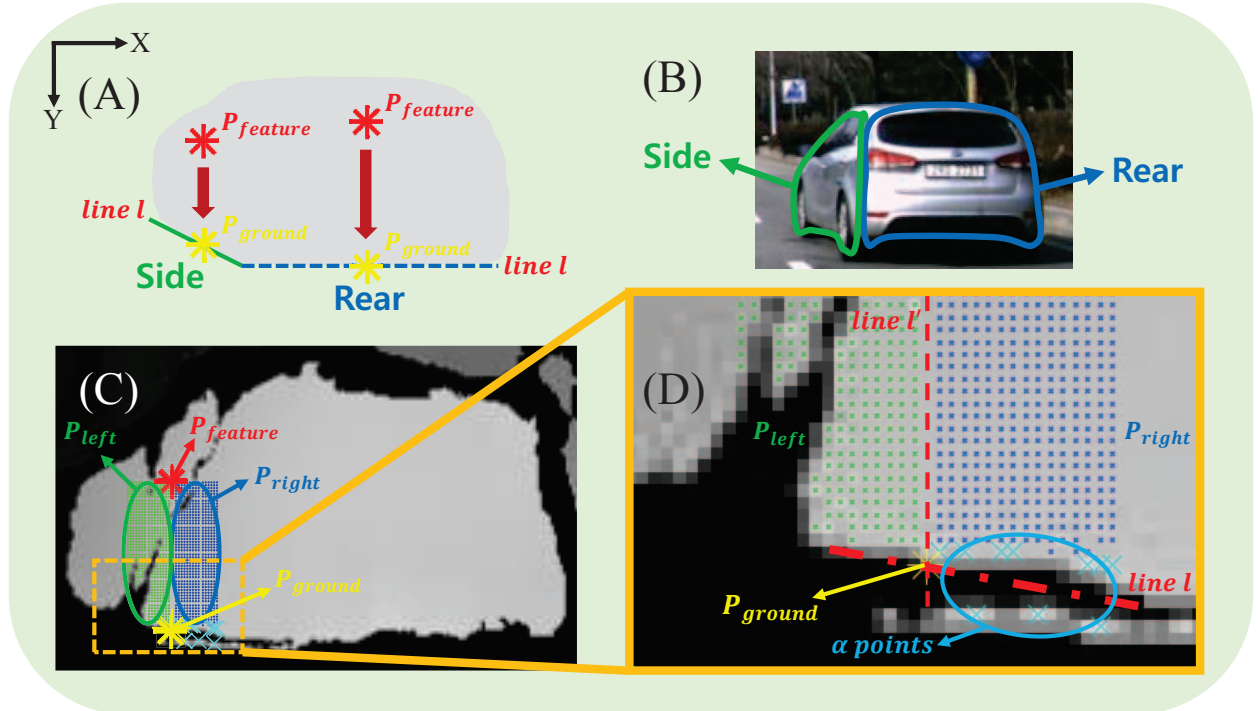


Figure 6. Schematic for grounded feature point formation algorithm. (A) Illustration of possible positions of a feature point. (B) Corresponding view of vehicle. (C) Schematic for grounded feature point formation on stereo depth map. (D) Magnified view of selected region.



Figure 8. Experimental results on vehicle detection and feature tracking. The top row shows vehicle detection results, and corresponding feature points (red) with grounded feature points (yellow) are shown on the bottom row.

IV. EXPERIMENTAL RESULTS

For collecting the input image data, VSTC-V200G stereo camera was mounted on a vehicle. The images from Fig. 8 exemplify experimental results on vehicle detection and feature tracking. As can be seen in Fig. 8, the proposed algorithm successfully detects partially occluded vehicles and corresponding features are found with various viewpoints.

To estimate the lateral position of surrounding vehicles, two scenarios (urban and highway settings) are considered. Fig. 9 shows the experiment outcomes from the two scenarios. The left two figures show that the slope and the y-intercept of the hough line fit to the v-disparity map are nearly constant for the two scenarios. This indicates that the ground detection is stable, which leads to the better performance of the grounded feature point formation algorithm. The right two plots of Fig. 9 are the results of lateral position estimation. For y-coordinates, pixel measure of the observed grounded feature point with IPM (Fig. 10) is converted to real world measure in meters. The lateral position is relative to the ego vehicle, which results in usage of local coordinate frames, and compared to the ground truth, which is manually obtained by measuring image pixels of identical vehicle part. The plots in Fig. 9 shows that the proposed method demonstrates robust performance and follows the true lateral position. Table I. summarizes the errors in approximating lateral position. Scenario 1 has a mean of about 1cm error and Scenario 2 has

a mean of less than 1cm error. These sum up to 0.00 m error for total frames, which is very ideal. This result is comparable to the work of [5] that uses the symmetry as the key feature for lateral position estimation. The result in this work has standard deviation error of 0.25m, and the proposed algorithm can detect lateral position regardless of viewpoint change and occlusion even when there is no symmetry.

TABLE I. ERRORS IN LATERAL POSITION ESTIMATION unit: m

	Scenario1	Scenario2	Total	[5]
Mean	-0.0103	0.0029	0.00	0.00
Standard Deviation	0.3055	0.1620	0.25	0.03

V. CONCLUSION AND FUTURE WORKS

In this paper, feature-based lateral position estimation algorithm is proposed using stereo vision. V-disparity, DCNN, and SVM are used for vehicle detection. Then, SURF, KLT, and IPM are utilized for feature tracking with a help of proposed grounded feature point. Lateral position estimation results in near zero mean error and 0.25m standard deviation error, and the algorithm works in various viewpoints and occlusion. Future work will focus on implementing the algorithm in dense traffic for multi-vehicle tracking and enable the system to work in real-time and non-planar road.

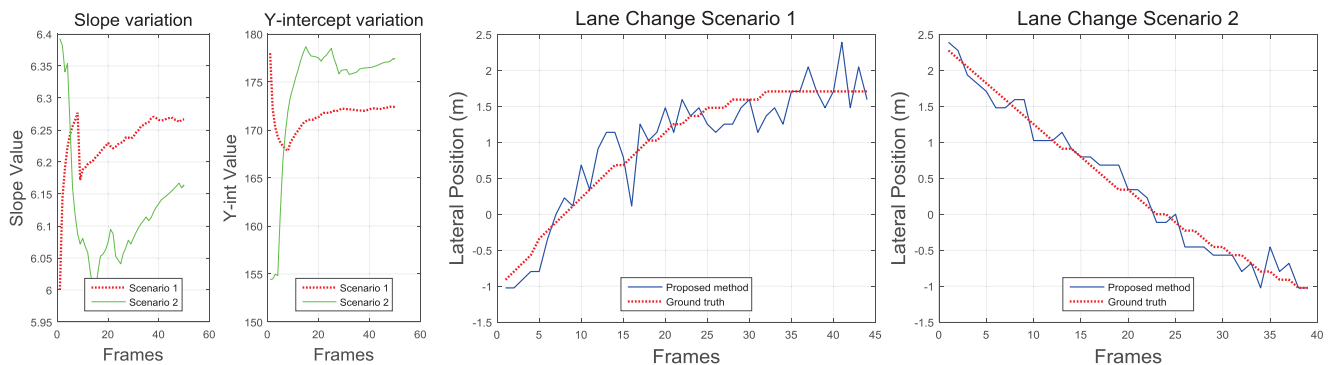


Figure 9. The slope and y-intercept values of hough line fit are shown on the left, and the lateral position estimation with ground truth is shown on the right.

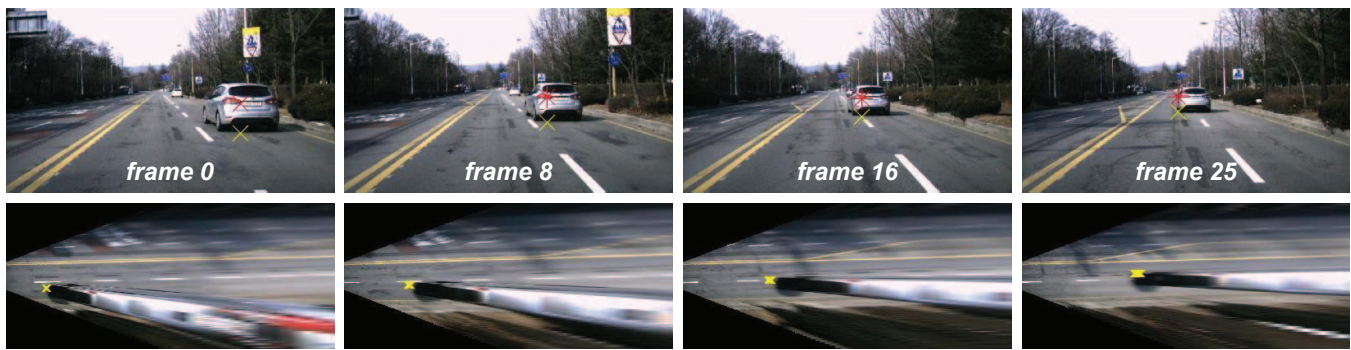


Figure. 10. Sequence of lane changing vehicle and lateral position estimation using inverse perspective mapping. Feature points (red) with grounded feature points (yellow) are shown on the top, and the grounded feature points with inverse perspective mapping (yellow) on the bottom are tracked over the frames.

ACKNOWLEDGMENT

This research was supported by the MSIP (Ministry of Science, ICT and Future Planning), Korea, under the ITRC (Information Technology Research Center) support program (IITP-2016-R2718-16-0011) supervised by the IITP (Institute for Information & communications Technology Promotion)

REFERENCES

- [1] J. Schlechtriemen, A. Wedel, J. Hillenbrand, G. Breuel, and K. Kuhnert, "A Lane Change Detection Approach using Feature Ranking with Maximized Predictive Power," *IEEE Intelligent Vehicles Symposium (IV)*, 2014, pp. 108–114.
- [2] S. Yoon and D. Kum, "The multilayer perceptron approach to lateral motion prediction of surrounding vehicles for autonomous vehicles," *IEEE Intelligent Vehicles Symposium (IV)*, 2016, pp. 1307–1312.
- [3] S. Sivaraman and M. M. Trivedi, "Looking at Vehicles on the Road: A Survey of Vision-Based Vehicle Detection, Tracking, and Behavior Analysis," in *IEEE Transactions on Intelligent Transportation Systems*, vol. 14, no. 4, pp. 1773–1795, Dec. 2013.
- [4] A. Mukhtar, L. Xia and T. B. Tang, "Vehicle Detection Techniques for Collision Avoidance Systems: A Review," in *IEEE Transactions on Intelligent Transportation Systems*, vol. 16, no. 5, pp. 2318–2338, Oct. 2015.
- [5] M. Nishigaki, S. Rebhan and N. Einecke, "Vision-based lateral position improvement of RADAR detections," *15th International IEEE Conference on Intelligent Transportation Systems*, 2012, pp. 90–97.
- [6] X. Wang, L. Xu, H. Sun, J. Xin and N. Zheng, "On-Road Vehicle Detection and Tracking Using MMW Radar and Monovision Fusion," in *IEEE Transactions on Intelligent Transportation Systems*, vol. 17, no. 7, pp. 2075–2084, July 2016.
- [7] R. K. Satzoda and M. M. Trivedi, "Efficient Lane and Vehicle Detection with Integrated Synergies (ELVIS)," *IEEE Conference on Computer Vision and Pattern Recognition Workshops (CVPRW)*, 2014, pp. 708–713.
- [8] R. K. Satzoda and M. M. Trivedi, "Multipart vehicle detection using symmetry-derived analysis and active learning," in *IEEE Transactions on Intelligent Transportation Systems*, vol. 17, no. 4, pp. 926–937, April 2016.
- [9] L. C. Chen, J. W. Hsieh, S. C. Cheng and Z. R. Yang, "Robust Rear Light Status Recognition Using Symmetrical SURFs," *IEEE 18th International Conference on Intelligent Transportation Systems*, 2015, pp. 2053–2058.
- [10] S. Liu, Y. Huang and R. Zhang, "Obstacle recognition for ADAS using stereovision and snake models," *17th International IEEE Conference on Intelligent Transportation Systems (ITSC)*, 2014, pp. 99–104.
- [11] B. Barrois, S. Hristova, C. Wohler, F. Kummert and C. Hermes, "3D pose estimation of vehicles using a stereo camera," *IEEE Intelligent Vehicles Symposium*, 2009, pp. 267–272.
- [12] F. Garcia, P. Cerri, A. Broggi, A. de la Escalera and J. M. Armingol, "Data fusion for overtaking vehicle detection based on radar and optical flow," *IEEE Intelligent Vehicles Symposium*, 2012, pp. 494–499.
- [13] R. Labayrade, D. Aubert, and J.-P. Tarel, "Real time obstacle detection in stereovision on non flat road geometry through "v-disparity" representation," in *IEEE Intelligent Vehicles Symposium (IV)*, 2002, pp. 646–651.
- [14] B. Tian, B. Morris and M. Tang, "Hierarchical and Networked Vehicle Surveillance in ITS: A Survey," in *IEEE Transactions on Intelligent Transportation Systems*, vol. 16, no. 2, pp. 557–580, April 2015.
- [15] Z. Sun, G. Bebis and R. Miller, "On-road vehicle detection: a review," in *IEEE Transactions on Pattern Analysis and Machine Intelligence*, vol. 28, no. 5, pp. 694–711, May 2006.
- [16] N. Bernini, M. Bertozzi, L. Castangia, M. Patander and M. Sabbatelli, "Real-time obstacle detection using stereo vision for autonomous ground vehicles: A survey," *17th International IEEE Conference on Intelligent Transportation Systems (ITSC)*, 2014, pp. 873–878.
- [17] S. Gehrig and U. Franke, "Stereovision for ADAS." Springer, 2015.
- [18] Y. Cai, X. Chen, H. Wang and L. Chen, "Deep representation and stereo vision based vehicle detection," *IEEE International Conference on Cyber Technology in Automation, Control, and Intelligent Systems (CYBER)*, 2015, pp. 305–310.
- [19] J. Yosinski, J. Clune, Y. Bengio, and H. Lipson, "How transferable are features in deep neural networks?," *Advances in neural information processing systems*, 2014.
- [20] Y. Zhou and N. Cheung, "Vehicle Classification using Transferable Deep Neural Network Features," *arXiv preprint arXiv:1601.01145*, 2016.
- [21] K. Chatfield, K. Simonyan, and A. Vedaldi, and A. Zisserman, "Return of the devil in the details: Delving deep into convolutional nets," *arXiv preprint arXiv:1405.3531*, 2014.
- [22] J. Arróspeide, L. Salgado, and M. Nieto, "Video analysis based vehicle detection and tracking using an MCMC sampling framework," *EURASIP Journal on Advances in Signal Processing*, vol. 2012, Article ID 2012:2, Jan. 2012.
- [23] D. Lowe, "Distinctive image features from scale-invariant keypoints," *International journal of computer vision* 60.2 (2004): 91–110.
- [24] H. Bay, A. Ess, T. Tuytelaars, and L. Gool, "Speeded-up robust features (SURF)," *Computer vision and image understanding* 110.3 (2008): 346–359.
- [25] S. Baker and I. Matthews, "Lucas-kanade 20 years on: A unifying framework," *International journal of computer vision* 56.3 (2004): 221–255.
- [26] D. C. Luvizon; B. T. Nassu; R. Minetto, "A Video-Based System for Vehicle Speed Measurement in Urban Roadways," in *IEEE Transactions on Intelligent Transportation Systems*, vol. PP, no. 99, pp. 1–12.
- [27] M. Bertozzi and A. Broggi, "GOLD: a parallel real-time stereo vision system for generic obstacle and lane detection," in *IEEE Transactions on Image Processing*, vol. 7, no. 1, pp. 62–81, Jan 1998.